ESR dating applied to optically bleached quartz - A comparison with 40Ar/39Ar chronologies on Italian Middle Pleistocene sequences

P Voinchet, A Pereira, S Nomade, C Falguères, I Biddittu, M Piperno, M-H Moncel, J-J Bahain

ESR dating applied to optically bleached quartz - a comparison with $^{40}Ar/^{39}Ar$ chronologies on Italian Middle Pleistocene sequences

P. Voinchet, A. Pereira, S. Nomade, C. Falguères, I. Biddittu, M. Piperno, M.-H. Moncel, J.-J. Bahain

PII: S1040-6182(20)30097-5

DOI: https://doi.org/10.1016/j.quaint.2020.03.012

Reference: JQI 8181

To appear in: *Quaternary International*

Received Date: 24 July 2018

Revised Date: 3 March 2020

Accepted Date: 6 March 2020

Please cite this article as: Voinchet, P., Pereira, A., Nomade, S., Falguères, C., Biddittu, I., Piperno, M., Moncel, M.-H., Bahain, J.-J., ESR dating applied to optically bleached quartz - a comparison with $^{40}Ar/^{39}Ar$ chronologies on Italian Middle Pleistocene sequences, *Quaternary International*, https://doi.org/10.1016/j.quaint.2020.03.012.

ESR dating applied to optically bleached quartz - a comparison with $^{40}Ar/^{39}Ar$ chronologies on Italian Middle Pleistocene sequences

P. Voinchet [1*], A. Pereira [1,2,3,4], S. Nomade [2], C. Falguères [1], I. Biddittu [5], M. Piperno [6], M.-H. Moncel[1], J.-J. Bahain [1]

[1]UMR 7194 HNHP – MNHN-CNRS-UPVD, ASU, Département Homme et Environnement, Muséum national d'Histoire naturelle, F-75013, Paris France
[2] Laboratoire des Sciences du Climat et de l'Environnement, UMR 8212 LSCE/IPSL, CEA-CNRS-UVSQ, Université Paris-Saclay, F-91191 Gif-sur-Yvette, France
[3] Ecole française de Rome, Piazza Farnese, IT-00186, Roma, Italy
[4] Sezione di Scienze Preistoriche e Antropologiche, Dipartimento di Studi Umanistici, Università degli Studi di Ferrara, C.so Ercole d'Este I, 32, Ferrara, Italy
[5] Italian Istitute of Human Paleontology, Piazza Ruggero Bonghi, 2, Anagni (FR), Italy
[6] Universita di Roma "La Sapienza", Dipartimento Scienze Storiche, Archeologiche e Antropologiche dell'Antichita, sezione di Paletnologia, Piazzale A. Moro, IT-00185 Roma (Italy)

* corresponding author - pvoinch@mnhn.fr

Abstract

The geological sequences of numerous Lower and Middle Palaeolithic sites of central and southern Italy, found in fluvio-lacustrine contexts and rich both in archaeological and palaeontological remains, have recorded various volcanic events all along the Middle Pleistocene timescale. These sedimentary sequences made of detritic and volcanic materials are suitable to compare independent numerical geochronological methods and thus develop a multi-method approach relying especially ESR method applied to optically bleached fluvial quartz and the $^{40}Ar/^{39}Ar$ on single grain isotopic method applied to potassium feldspars. In this present paper, geochronological data obtained using these two methods were used on several Middle Pleistocene Italian sites including volcanic and fluvial but also archaeological levels: Isoletta and Lademagne in Lazio and Notarchirico in Basilicata. In this contribution, ESR age estimates were performed using a multi-centre approach from Al, Ti-Li and Ti-H centres. We demonstrate for these sites that ESR-based framework is overall consistent with the $^{40}Ar/^{39}Ar$ chronology that over the 700 and 350 ka time window. This comparison validates the multi-centre approach proposed and demonstrates that the use of Ti-H for samples with equivalent doses higher than 280-300 Gy leads to systematic age underestimates.

Keywords: ESR dating, optically bleached quartz, $^{40}Ar/^{39}Ar$ dating, Middle Pleistocene Italian sites

1. Introduction

Since the mid-1990s, Quaternary river deposits have been the subject of in-depth multidisciplinary studies, including systematic dating. This kind of research, partly initiated by a team of researchers from the Muséum National d'Histoire Naturelle (MNHN) in Paris, France, has led to the electron spin resonance (ESR) dating of stepped and embedded terrace systems for a large number of valleys in Europe and Asia (e.g., Laurent et al., 1994, 1998; Voinchet et al., 2004, 2010, 2013; Despriée et al., 2011). These numerous works have contributed to establish a detailed chronostratigraphic framework for these river sequences covering most of the Pleistocene. Associated with some of these fluvial formations, tens of Palaeolithic localities with lithic assemblages have also been dated by the same way. The results obtained for each valley are consistent with each other, producing a robust geochronological framework, although there is often no independent age control available so far. Indeed, due to the nature or the chronology of the studied sedimentary sequences, ESR dating of quartz grains has been for a long time one of the very few numerical dating methods that could be used. In some area, the absence of fossil faunal remains, linked to the extreme acidity of quartz sands, precludes any biochronological estimation for the archaeological localities, as well as the use of the ESR/U-series method applied to teeth. In addition, the fluvial sediments are often coarse and unconsolidated and therefore not suitable for magnetostratigraphic analysis (Parés et al. 2013). Finally, the application of luminescence dating of sediments using standard procedures (OSL, IRSL, TL) was long limited to Middle and Upper Pleistocene deposits (Arnold et al., 2003). As a result, for a long-time alternative dating estimates derived from independent methods has not been possible for the oldest deposits and sites of these valleys. Although recent methodological developments have shown that a multi-technique dating approach can now be confidently envisaged to date Early to Middle Pleistocene fluvial deposits (e.g., Duval et al., this volume) this overall lack of independent age control is considered by many as prejudicial. Its casts doubt on the relevance of the obtained chronology, for example regarding the exact period of arrival of the first human migration in Western Europe (Muttoni et al., 2013, Muttoni et al., 2018)

Fortunately, the particular case of central and southern Middle Pleistocene river sequences in central and southern Italian peninsula, where fluvial deposits include K-rich volcanic material, allows the

straightforward comparison between ESR and an independent reference radioisotopic method, $^{40}Ar/^{39}Ar$. Indeed, in this area, the presence of numerous volcanoes, active during the Middle Pleistocene and located mainly along the Tyrrhenian margin, has led to the emission of large and widespread tephra. In consequence, volcanic materials are frequent into sedimentary sequences, sometimes as primary tephra layers interspersed into the sequences or mixed with fluvial deposits. In this case, the volcanic materials are not in primary position (i.e. within a volcanic deposit) but reworked, sometimes by the river (secondary position). In this case, $^{40}Ar/^{39}Ar$ studies show the presence of grain populations of various ages, the youngest being considered as the last volcanic event locally recorded before the deposition of the analysed sediment. In other words, volcanic material could be considered either as linked to a primary deposition or as a secondary one indicating the last volcanic event recorded in the area. In central and southern Italy, such volcanic materials recovered in primary or secondary position were dated by $^{40}Ar/^{39}Ar$ allowing the establishment of a robust and precise chronostratigraphic framework (e.g., Pereira et al., 2018).

This framework offers the possibility to a comparison between palaeodosimetric and radio-isotopic results. In the present contribution, we will compare ESR ages obtained on quartz using the multi-centre method (ESR-MC) with $^{40}Ar/^{39}Ar$ dates on single feldspar grains in order to evaluate (i) the accuracy of the ESR results and (ii) the reliability of the ESR-MC approach. Of course, it is worth noticing that such comparison is only possible if stratigraphic knowledge of the sampling levels confirms the sub-contemporaneity of the studied geological layers and of the evidenced volcanic events. At the end, it should permit to improve the chronology of the studied sequences and, if the data agree, to reinforce the robustness of the general chronological framework.

2. ESR dating method

Methodological developments in the ESR dating of optically bleached quartz grains over the two last decades have made it a reference method for the dating of Quaternary fluvial deposits (Antoine et al., 2007; Chauhan et al., 2017). Among these developments, one of the most important is the use of the so-called multiple centre (MC) approach based on the study of several light-sensitive paramagnetic

centres in quartz (Toyoda et al; 2000, 2006; Tissoux et al., 2007; Duval and Guilarte, 2015; Duval et al., 2015).

Concerning the ESR dating of sedimentary quartz grains found in alluvial terrace deposits, it is essential that a "reset" of the geochronometers (here, the paramagnetic centres) occurred before sediment deposition. Such reset is essential in order to date this deposition event and not the formation of the quartz itself. This reset depends on the exposure to UV sunlight and is called optical bleaching. It occurs during river transport before the deposition of the sediment (Yokoyama et al., 1985; Voinchet et al., 2003; Voinchet et al., 2007). The main challenge for the ESR dating method lies in the estimation of the bleaching rate of the analyzed quartz grains during the transport, which may significantly varies among centres. The ESR-MC method is based on the systematic measurement of both aluminum (Al) and titanium (Ti) centres (mainly, Titanium-Lithium (Ti-Li) and Titanium-Hydrogen (Ti-H)) in a given quartz sample.

The Al centre has long been the most widely used in ESR dating of quartz (Voinchet et al., 2004) because aluminum is particularly abundant in this mineral and the corresponding ESR signal is easily measured and observed. In addition, this Al-centre has a long-life expectancy due to a thermal stability (for temperatures below 100°C) that exceeding six million years (Toyoda et al, 1991). It can thus be used to date samples as old as several million years (Laurent et al., 1998; Gouveia et al., 2020). Nevertheless, the fact that this centre requires a long exposure to light to be bleached (about 1600 hours – Toyoda et al, 2000; Voinchet et al, 2003) and the fact that, even after such a long exposure, a residual ESR signal is still observed, can sometimes be problematic. Indeed Al-centre is partially optically bleached and its signal intensity decreases in relation to time exposure to solar light, until it reaches a plateau value corresponding to a residual signal attributed to “Deep Aluminium Traps” (DAT) (Tissoux et al 2013). These traps or centres cannot be reset by an exposure to sunlight. A wrong estimation of the ratio between DAT and OBAT (Optically Bleachable Aluminium Traps) can lead to a wrong estimation of the equivalent dose D_E and by extension of the age.

In comparison, the Ti centres are less frequently observed in quartz samples and their ESR intensities may be significantly smaller than those of the Al centre. For dating, two Ti centres can mostly be used, the Ti-Li and Ti-H centres. These two centres have signals that are much more light-sensitive than the

Al and which therefore usually totally reset during sediment transport. Typically, Ti-H centre can be zeroed or bleached within a day, while Ti-Li centre needs about 20 days for the complete zeroing (Toyoda et al., 2000; Rink et al., 2007; Tissoux et al., 2007). However, Ti-H is also much more radiosensitive than the Al and Ti-Li centre and saturates much faster (Duval and Guilarte, 2015). Consequently, the Ti-H centre is usually considered as more suitable for small equivalent dose estimates (few grays to tens of grays) and/or for recent samples (Miallier et al., 1994) between tens of thousands of years (ka) and a few hundred of ka. The joint use of the Al and Ti centres, or MC approach, is therefore intended to better estimate the quality of the sediment bleaching during transport. This approach has been used several times in recent years, and several studies have shown its potential in a variety of sedimentary contexts and for periods ranging from the Lower to the Upper Pleistocene (Bartz et al. 2018, Duval et al. 2015, this volume; Gouveia et al. 2020; Kreutzer et al. 2018;).

3. Sampling

Three Italian archaeological sites were sampled in the frame of this work: Isoletta and Lademagne sites in Lazio and Notarchirico in Basilicata (Fig.1). In order to limit the risks of bad bleaching, linked to a transport of the quartz grains in opaque water, the fluvial sediments sampled for ESR dating are made of fine sands without silt or clay in the matrix (Voinchet et al, 2015). These sediments have been carried by clear water river, without any fine particles in suspension.

All of the analyzed geological levels correspond to fluvial deposits, containing fine quartz grains and characterized by the occurrence of volcanic minerals, allowing the use of the $^{40}Ar/^{39}Ar$ single crystal approach. The $^{40}Ar/^{39}Ar$ isotopic technique is one of the most accurate and precise dating methods available for Middle Pleistocene time range (Pereira et al., 2015; 2018). In fact, the individual dating of volcanic crystals allows the identification of the corpus of volcanic events reworked and drained in sedimentary layers. In a geological layer, the juvenile crystals population highlighted by the related probability diagram gives chronological information on the age of the youngest volcanic event reworked (see Pereira et al., 2015, 2018 for further explanations). The uncertainties obtained on the calculated ages are ranging between 1 to 5 % (2σ analytical uncertainty).

The volcanic materials found at Isoletta and Lademagne sites are originated from the nearby volcanic complexes of Colli Albani or Ernici mounts (Pereira et al., 2018), whereas at Notarchirico they derived from the mount Vulture stratovolcano activity (Lefèvre et al., 2010; Pereira et al., 2015).

3.1 Isoletta site

Isoletta is located in the Ceprano tectonic basin at the confluence of the Liri and Sacco Rivers, near the town of Pofi in the Frosinone Basin, few kilometres south-east of the Campogrande/Ceprano *Homo heidelbergensis* site location (Fig. 1). It displays a typical alluvial terrace stratigraphic sequence, particularly thick (more than 30 m) (Fig.2. and 5). This sequence was punctually exposed thanks to the high-speed train railways construction and was sampled in 2000. Three main units were then individualized: gravels at the base, overlain by very fine sediments (silts and clays) rich in organic matter and finally an alternation of medium to coarse sand beds over more than 10m (Fig.2). In this sequence, two archaeological levels were identified (Fig.2): the first one in basal gravels, is characterized by the presence of Mode 1 lithic (cores-and-flakes type) and bones industries while the second one, in a sandy layer of the upper unit, has displayed Mode 2 (Acheulean) lithic artefacts and "Galerian" faunal assemblage (corresponding to the first half of the Middle Pleistocene) (Biddittu, 1974, Sardella et al., 2006).

The gravel level at the bottom and the sand levels of upper sequence are very rich in reworked volcanic material (Fig.2.). Four samples were taken from different levels for ESR dating: the first in the coarse level of the base (ESR 1) and the three others (ESR 2, 3 and 4) in three decimetre-thick medium to fine sand beds showing fluvial sedimentation features. ESR 2 sample corresponds to the higher archaeological level ("Acheulian level", see GA6Z, Pereira et al., 2018). The basal part of the sequence as well as the levels having provided ESR2 and ESR4 contain volcanic minerals (potassium feldspars) that have been dated by $^{40}Ar/^{39}Ar$. The $^{40}Ar/^{39}Ar$ dated feldspars of this sequence are in secondary position (it is not a tephra level but a fluvial deposit). This means that the age of this deposit may be similar or younger than the $^{40}Ar/^{39}Ar$ estimate. Nevertheless, the $^{40}Ar/^{39}Ar$ age is constrained by the higher levels in the stratigraphy which indicate that the river uptake of these volcanic minerals occurred shortly after their primary deposit (Pereira et al, 2018).

178 3.2 Lademagne site

179 Lademagne site, located 5 km from Isoletta in the Ceprano tectonic basin was discovered in 1965 (Fig.
180 1). The stratigraphic sequence is mainly composed of sandy-gravelly deposits inter-bedded with
181 volcanic rich sediments (Fig.3) and is very similar to the upper part of Isoletta's sequence. Two
182 archaeological layers with both Mode 2 industries are mentioned in the literature (Biddittu et al., 2012)
183 and present palaeontological and archaeological assemblages close to those of Isoletta upper level
184 (Biddittu et al., 2012). One sample was taken for ESR dating at the top of the stratigraphy (named Lad
185 Sup) and can be compared with one sample taken in the same level for $^{40}Ar/^{39}Ar$ dating on single
186 crystal (named also Lad Sup in Pereira et al, 2018). As at Isoletta, the feldspars of this sequence are in
187 secondary position and provide therefore maximum ages to the sediment deposition.
188
189 3.3 Notarchirico
190 Discovered in 1979, Notarchirico site is an Early Middle Pleistocene site of the Venosa basin (Fig.1.)
191 (Piperno et al., 1999). The sequence is seven metres thick and is mainly composed of volcanoclastic
192 sediments deposited and reworked in a fluvial environment. Many stratigraphical levels are rich both
193 in volcanic materials coming from the close Monte Vulture stratovolcano and quartz transported by
194 the river (Fig.4. and 5).
195 The site is characterized by the record of repeated periods of human occupation, most part of them
196 linked to butchery activities. A total of eleven archaeological layers (Fig. 5. Piperno et al., 1990, 1999)
197 have been identified (Piperno and Tagliacozzo, 2001). One femur attributed chronologically to *Homo*
198 *heidelbergensis* has been discovered in the upper part of the sequence and some of the archaeological
199 levels (levels A, A_1, B, D and F) contain bifaces referred to Mode 2 technology (Piperno and
200 Tagliacozzo, 2001).
201 Three levels have been sampled at Notarchirico, one in the middle part of the sequence (level 2-6,
202 Notarchirico 2-6 sample) and two in the newly investigated lower part (level H1 and H1c,
203 Notarchirico H1 sample and Notarchirico H1c sample) (Fig.4. and 5). For now, only level 2-6 has
204 been dated by ESR applied on quartz (Al) and $^{40}Ar/^{39}Ar$ methods (Pereira et al., 2015) applied on

secondary deposit feldspars. It should be noticed that level 2.4 located between levels 2-6 and H1-H1c corresponds to a tephra in primary position.

4. Material and method

4.1 ESR dating

Sediment samples were prepared according to the procedure used in the Muséum National d'Histoire Naturelle (MNHN) laboratory (Voinchet et al, 2004). Firstly, the 100-200 µm grain size fraction, the most easily bleached during river transport (Voinchet et al. 2015), was collected by wet sieving. The organic matter was removed by an attack with hydrogen peroxide (30%) and the carbonates were destroyed using hydrochloric acid (36%). After ultrasonic use, in order to break the weaken minerals with cleavage plane, the samples were then attacked with HF (40%) during 1h 40min to firstly destroy the feldspar grains and then to remove the external part of the quartz grains. We observe that the etching effect varies in thickness between 10 to 20 µm depending of the grain shape. Recent works have demonstrated that the previously recommended 40min-long attack was sometimes not enough to remove all the feldspar grains, especially in case of very feldspar rich sediments (Tissoux et al, 2017). A new HCl attack eliminates then the fluorides formed during this etching. The heavy minerals and the magnetic minerals are then removed with a sodium polytungstate heavy liquor at d=2.72 g/ml and with magnets respectively.

The quartz grains thus separated were dated using the Multiple Aliquots Additive Dose (MAAD) method. Each sample was divided into 11 aliquots (each one, around 100 mg, composed by several thousand grains). Nine of them were irradiated using a ^{60}Co source (CEA, Saclay) with a dose rate of 260 ± 20 Gy/h. The following doses were applied to these aliquots: 264, 431, 653, 1048, 1663, 2640, 4460, 8010, 12500 Gy. In order to evaluate the residual non-bleachable ESR signals from the Al centre, one aliquot was exposed to a SOL2 sunlight simulator (Dr Hönle) for about 1600h. The last aliquot (natural aliquot) was neither irradiated nor exposed to sunlight.

All aliquots were then measured by ESR at the MNHN dating laboratory (Paris, France), using an EMX Bruker X-band spectrometer with a high sensitivity spherical cavity. These measurements were performed at low temperature (~100 K) by cooling the cavity with liquid nitrogen.

To apply the multi-centre method as defined by Toyoda et al (2000), the ESR signal intensities of the Al and Ti centres (Ti-Li and Ti-H) were measured. The ESR intensities of these different centres were measured on a single spectrum (fig.6) using the following acquisition parameters: a 5 mW microwave power, 1024 points resolution, 20 mT sweep width, 100 kHz modulation frequency, 0.1 mT modulation amplitude, 40 ms conversion time, 20 ms time constant. Two cumulative scans were performed to reduce background noise on the Ti signals. The signal intensity of Al centre was measured between the top of the first peak at g=2.018 and the bottom of the 16^{th} peak at g=1.993 (fig.6) of the Aluminum hyperfine structure (Toyoda and Falguères, 2003). The ESR intensity of the Ti-Li centre was determined by measuring the difference between the peak top (g= 1.913) and the baseline (Toyoda et al, 2006, Tissoux et al, 2007, Duval et Guilarte, 2015), while the intensity of the Ti-H centre was measured between the peak apex (g= 1.917) and the baseline (fig.6) (Toyoda et al, 2006, Tissoux et al, 2007, Duval et al, 2015).

Due to the angular dependence of the signal, linked to the heterogeneity of the grains orientations in the ESR magnetic field, each aliquot of a given sample was measured 3 times after a tube rotation of about 120° of its initial position in the cavity. In addition, the measurements were repeated three times on different days to test the repeatability of the measured intensities and as a result of the equivalent dose obtained. As a result, nine intensities were obtained for each measured signal (Ti-Li, Ti-H and Al) in each aliquot of all quartz samples studied. ESR intensities are calculated using the average of the nine measurements. The variation between the nine intensities of each aliquot measured on the three days does not exceed 5%. If a measurement exceeds this percentage, it was removed from the calculation, and a new measurement was made to determine if the previous value was due to a one-time event.

For Al signals, the value of the ESR intensity of the bleached aliquot was systematically subtracted from the ESR intensities of the other aliquots to account the centres that cannot be bleached by light (DAT, Tissoux et al., 2012). The bleaching rate δ_{bl} (%) is then determined by comparison of the ESR intensities of the natural and bleached aliquots ($\delta_{bl}= ((I_{nat}-I_{bl})/I_{nat})x100$).

After normalization of ESR intensities by aliquot mass and receiver gain, the equivalent doses (D_E) were then determined from the averaged ESR intensities using a coupled exponential and linear fitting

function (E+L) for Al and Ti-Li (Duval et al, 2009, Duval, 2012; Voinchet et al., 2013). By limiting the curve to the first six points (from natural to the 1663 Gy point) it is also possible to use a single saturating exponential function for the Ti-Li D_E determination. For Ti-H centre, due to the shape of growth curve (fig.7), we tested two functions (fig 7.), Ti-2 function by considering all the data points, and single saturating exponential (SSE) one by considering only the points of the curve corresponding to its increasing part (from natural to the 1663 Gy point).

Dose response curve fitting and D_E evaluation was performed using with Microcal OriginPro 8 software with $1/I^2$ weighting

The dose rate (D_a) determined from the sum of the alpha, beta, gamma and cosmic-ray contributions. Gamma dose rate was determined by *in situ* measurements directly at the sampling point using an Inspector 1000 gamma spectrometer (Canberra©), except for the Isoletta section sampled in 2000, i.e. before the systematic use by our team of gamma spectrometer on the field, and now not yet accessible. These *in situ* gamma doses were estimated using the threshold approach (Mercier and Falguères 2007). External alpha and beta contributions were calculated from the sediment radioelement contents (U, Th and K) as determined in the laboratory by high resolution and low background gamma-spectrometry. The internal dose rate was considered as negligible because of the low contents of radionuclides usually found in quartz grains (e.g., Murray and Roberts 1997; Vandenberghe et al. 2008). Age calculations were performed using the dose-rate conversions factors from Guérin et al (2011) and a k-value of 0.15 ± 0.1 (Yokoyama et al., 1985). Alpha and beta attenuations estimated for the selected grain sizes (100-200µm) from the tables of Brennan et al., (1991) and Brennan (2003) respectively. Alpha contribution takes account of an etching of 10 to 20µm of the grains. This difference of 10µm in the thickness removed by the acid attack induces an age variation of 1 to 2% depending on the samples and on its radioactive environment. Water contents (W%) were estimated by the difference in mass between the natural sample and the same sample dried for a week in an oven at 50°C and water attenuation were then determined using formula from Grün (1994). The cosmic dose rates were calculated from the equations of Prescott and Hutton (1994). ESR age estimates are given with one sigma error range. The doses rate and ages were calculated using a specific Microsoft © Excel template including data mentioned previously.

When Al and Ti results agree with 1σ, weighted average ages combining the different ESR centres, were calculated using IsoPlot3.0 (Ludwig, 2003). Mean Square of Weighted Deviates (MSWD) and Probability (P) are then given for each result.

4.2 $^{40}Ar/^{39}Ar$ analyses

The single crystal dating using $^{40}Ar/^{39}Ar$ isotopic method is actually one of the most accurate methods available for Middle Pleistocene time range (Pereira et al., 2015; 2018) and gave us the possibility to date and identify the volcanic events recorded in sedimentary layers. In central Italy, the studied deposits could contain minerals such as sanidines or feldspathoïds leucites that have up to 11 to 18 % of K. We therefore use mainly these minerals to establish our $^{40}Ar/^{39}Ar$ chronology (see Pereira et al., 2015, 2018). The analytical protocols followed and the details about the $^{40}Ar/^{39}Ar$ ages mentioned in this study were presented in details in Pereira et al. (2015, 2018) or Moncel et al. (2018). All $^{40}Ar/^{39}Ar$ ages discussed hereafter are calculated using the potassium total decay constant of Steiger and Jäger (1977) and the monitor standard ACs-2 dated at 1.193 Ma. We are fully aware than other calibrations exist such as the total decay constant of Renne et al. (2011) and the ACs-2 at 1.1891 Ma (e.g. Niespolo et al., 2017) but there is not matter for the purpose of this article, considering that the implied age difference of ≤ 1% is negligible compared to the uncertainties of the ESR method. We therefore in the scope of this contribution do not discuss the various parameters than can be used to calculate $^{40}Ar/^{39}Ar$ ages. These ages are given with 2σ analytical uncertainty.

5. Results and discussion

U, Th and K concentrations of the different sediment samples are shown in table 1 and external dose rates (alpha, beta gamma and cosmic doses), water contents (W%), bleaching rates (Bl%), and equivalent doses with indication of the quality of the ESR growth curve fitting (r^2) are given in table 2.

5.1. ESR results: general comments

316 The Al centre could be measured in all our samples. Similarly, the Ti-Li centre was measured for
317 almost all these samples, with the exception of Notarchirico 2-6. For this sample, Ti signal intensity
318 was too weak and too close to background noise to be reliably evaluated, even with two scans. It is
319 worth noticing that if Ti signal intensity is extremely low for Notarchirico 2-6 quartz sample, this was
320 not the case for the other Notarchirico samples from levels H1 and H1c, for which the use of multi-
321 centre approach was therefore possible.
322
323 For Ti-Li, the equivalent doses (D_E) were determined following two different approach: firstly, using
324 a coupled exponential and linear fitting function (E+L) (Duval et al, 2009, Duval, 2012; Voinchet et
325 al., 2013). Secondly using a single saturating exponential function by limiting the curve to the first six
326 points (from natural to the 1663 Gy point). The results of the two approaches are relatively similar and
327 are presented in Table 2. We have chosen to use the doses determined using the E+L function for the
328 age calculation. However, since the intensity of Ti-Li does not decrease for high doses, we did not use
329 the Ti-2 function proposed by Duval and Guilarte (2015).
330 The Ti-H centre has only provided useful results for samples from Isoletta and Notarchirico H1 and
331 H1c levels. The Ti-H signal frequently shows a signal-to-noise ratio lower than that of Al or Ti-Li
332 signals, and it is sometimes impossible to obtain meaningful ESR intensities. It is the case for the
333 Lademagne sample for which Ti-H signal cannot be differentiated from the background ESR noise.
334 The shape of the curves led us to test two different approaches for the determination of D_Es, firstly,
335 using the Ti-2 fonction (Duval et Guilarte, 2015) by considering all the data points, and secondly using
336 a single saturating exponential (SSE) by considering only the points of the curve corresponding to its
337 increasing part (lowest added doses, between natural and 1663 Gy).
338 For this Ti-H centre, the D_E values obtained using SSE and Ti-2 functions are quite identical and
339 within 1-σ error (table 2), except for one sample (ESR3). Consequently, the choice of the fitting
340 function has a very limited impact on the dose estimates. The results are extremely close and we have
341 chosen to use only the SSE results, which after Woda and Wagner (2007) describe more the physical
342 filling phenomenon of ESR centres. Consequently, final Ti-H ESR age estimates were therefore
343 calculated in the present study using the SSE function D_E.

344

345

346 5.2 Isoletta

347 At Isoletta, the $^{40}Ar/^{39}Ar$ ages of the levels containing tephra constrain the deposition of river
348 sediments between 403 and 365 ka. The ESR results obtained from Ti-Li and Al centres are consistent
349 within 1σ with the available $^{40}Ar/^{39}Ar$ ages, with the exception of sample ESR 1. For this sample, the
350 three centres give very different and clearly overestimated results, indicating both a poor bleaching of
351 Al and Ti-Li centers – at least – and raises questions abour the dose rate evaluation (Tab. 3).
352 For ESR2 sample, the use of Ti-H centre provides strongly younger ages, while, for ESR4 and ESR3
353 the three ages are close and coherent with $^{40}Ar/^{39}Ar$ ages. For these two samples, the equivalent doses
354 obtained using both Al and different Ti centres are lower than 300 Gy. In contrast, the Ti-H yields
355 much smaller De values compared with Al and Ti-Li when De values >1,000 Gy, i.e. for sample ESR
356 2. Leaving aside the possibility of incomplete bleaching of the Al and Ti-Li signals, this would suggest
357 that the Ti-H centre tends to saturate for doses above 300-400 Gy and cannot provide reliable dose
358 estimates above this dose. These results agree with previous observations (Tissoux et al, 2007; Duval
359 and Guilarte 2015).

360

361 The relatively large error ranges observed for these ESR ages originate from the D_E evaluation, and are
362 explained by a relatively poor goodness-of-fit achieved for the dose response curves, with r^2 values
363 sometimes lower than 0.99 (Tab 2). For Isoletta samples when D_E values obtained using the different
364 centres were similar, a weighted average age was calculated for the corresponding level. Such
365 weighted average ages were calculated using IsoPlot 3.0 (Ludwig, 2003) and given at 95 % of
366 confidence.
367 For ESR 3 and ESR 4 samples, the weighted average age was calculated using the three different
368 centres, while Al and Ti-Li ages were used for ESR 2 sample.
369 Weighted mean ages of 442 ± 58 ka (2σ, Full external error, MSWD = 0.65 and P = 0.42) 349 ± 26 ka
370 (2σ, full external uncertainty, MSWD = 2.08 and P = 0.059) and 396 ± 41 ka (2σ, full external error,

MSWD = 0.27 and P = 0.76) were obtained for Isoletta ESR2, ESR3, associated to the "Acheulian level", and for Isoletta ESR4 samples, respectively.

The ESR age estimates of Isoletta ESR1 sands seems overestimated compared with $^{40}Ar/^{39}Ar$ results, whatever the centre considered. In addition, the significant discrepancy between Ti-Li and Al age results precludes the calculation of a weighted mean age value, and the fact that the Ti-Li D_E and age are higher than the Al ones

We suspect here an overestimation of the natural signal, related to the difficulty of accounting for background noise and baseline in the case of extremely weak signals. This overestimation directly leads to an overestimation of the D_E. The discrepancy between the ages obtained using the different centres does not allow as the determination of reliable depositional age for this sample.

The fact that we observe also a very clear age overestimation using Ti-H for this sample leads us to suppose that the problem may also be related to the annual dose evaluation rather than to only a poor initial bleaching of the quartz grains. Indeed, this level is composed of very coarse elements (blocks, pebbles...) whose sandy matrix constitutes the dated sediment. The absence of an *in situ* gamma measurement means that coarse elements (the main part of the sediment in the level) were not taken into account when determining the annual dose, which could explain the results obtained for this level. It should also be noted that the Th and K content of the sediment sample at this level is extremely low (0.31 ppm and 0.03% respectively; Table 1). For K, an alteration (disappearance) of the potassium-rich minerals (feldspar?) all along the time elapsed between the sediment deposit and the sampling could explain this low content, leading to an underestimation of the annual dose and by extension an overestimation of the age.

5.3 Lademagne

For the sediment from Lademagne upper level, the Ti-H ESR signal was not measurable. The ESR ages using Ti-Li (398± 51 ka) and Al (406± 51 ka) centres are consistent (table 4). As for the main part of Isoletta's samples, the close D_E obtained using the Ti-Li and Al centres allows us to give a weighted average age of 402 ± 71 ka (2σ, Full external error, MSWD = 0.012 and P = 0.91) for these upper sands. This result agrees with the $^{40}Ar/^{39}Ar$ age (389 ± 8 ka) obtained for the same sediment.

However, in this case, several grain populations showing different ages have been identified, indicating that the volcanic minerals are not in primary position. Consequently, the $^{40}Ar/^{39}Ar$ age of 389 ± 8 ka should be interpreted as a maximum age constraint for the deposits, as it was derived from seven crystals showing the most recent ages (Pereira et al, 2018). The corresponding volcanic event being not recorded in the Lademagne lower level sediment in which the youngest recorded eruption was dated of 405 ± 9 ka (Pereira et al, 2018), we can however consider in first approximation that it probably happened shortly before the upper level deposition.

5.4 Notarchirico

Only level 2-6 can be directly compared with an $^{40}Ar/^{39}Ar$ result (663 ± 3 ka). However, this level is considered as a secondary deposit, as volcanic minerals seems derive from the reworking of the Notarchirico tephra (level 2.2), the only one real primary deposit of the sequence, located about 60 cm lower in the sequence and directly dated to 661 ± 3 ka (Pereira et al, 2015). The Al ESR age of Notarchirico 2-6 sample (657 ± 31 ka) agrees at 1σ with the $^{40}Ar/^{39}Ar$ obtained on the youngest volcanic event reworked into this level. No crystals resulting from a younger eruption dated about 614ka and recorded in the upper levels of the sequence are present in level 2-6. The age of this deposit is therefore strictly constrained between 661 and 614 ka.

For samples from H1 and H1c levels, the three ESR centres have been measured. As for the Isoletta site, the ESR ages obtained using the Ti-Li and Al centres are consistent with each other and with the $^{40}Ar/^{39}Ar$ ages (table 4) of the neighboring levels, whereas the Ti-H ages are significantly younger. This result is probably related to the high D_E values (> 400 Gy) and the probable aforementioned Ti-H centre saturation. The close D_E values obtained for the Al and Ti-Li centres led to weighted mean ages of 743 ± 67 ka (2σ, Full external error, MSWD = 0.024 and P = 0.88) and 736 ± 70 ka (2σ, Full external error, MSWD = 0.013 and P = 0.91) for Notarchirico H1 and Notarchirico H1c samples, respectively. We can also notice that the Al and Ti-Li ESR ages obtained for the lower levels of the Notarchirico sequence are significantly older than the date determined for level 2-6. Nevertheless, as quite the whole sequence (levels J to B) was developed within the same climatic stage according to the palaeoenvironmental data (that $^{40}Ar/^{39}Ar$ dates place during MIS16, Pereira et al., 2015 and as the

error range of the ESR ages is relatively wide, the ages of levels H1 and H1c can be compared with the $^{40}Ar/^{39}Ar$ results of 670 ± 3 ka (Pereira et al., 2015) obtained for level F (table 5). This result then sets a minimum age limit for H levels. ESR results may seem incoherent with this estimate, but considering the error range associated with ages, this is still consistent with it. Moreover, the results of the H1 levels are much older than the $^{40}Ar/^{39}Ar$ ages of the levels that cover them. Nevertheless, the estimated $^{40}Ar/^{39}Ar$ ages obtained for F levels gave minimum ages for H1 and H1cand therefore do not disagree with those actually obtained by ESR for these levels. It would be desirable in the future to constrain this chronology by $^{40}Ar/^{39}Ar$ dating of sanidines extracted from these lower layers.

6. Conclusion

A multi-centre ESR approach was used on quartz grains extracted from Middle Pleistocene fluvial deposits of central Italy that were also dated by the $^{40}Ar/^{39}Ar$ method. For most of the samples analyzed, except one sample from the Isoletta site (ESR1), the ages determined both from Ti-Li and Al signals are in agreement with each other and consistent with the $^{40}Ar/^{39}Ar$ ages (Fig. 8). As mentioned in previous works, the use of the Ti-Li centre is therefore appropriate for this time range (Tissoux et al, 2007; Duval et Guilarte, 215) andthis use is here validated by comparison with a totally independent method, based on totally different physical principle. Furthermore, the results derived from Al signal clearly show the usefulness of this centre when the fluvial sediments sampled are made of fine sand carried by clear water river (without any fine particles in suspension). An evidence of this transport condition is showed by the absence of silt or clay in the sampled sandy layers.

Our results strengthen the validity of ESR-MC method to accurately date sedimentary successions in fluvial context proposed in previous studies (Tissoux et al, 2007; Bartz et al. 2018, 2019; del Val et al. 2019; Duval et al. 2015, 2017, this volume; Gouveia et al. 2020; Kreutzer et al. 2018; Mendez Quintas et al. 2018; Sahnouni et al. 2018). The only discordant sample, Isoletta ESR1, was carried out from extremely coarse and poorly sorted sediments probably of colluvial origin, in which quartz grains could not have been completely bleached,

or in relation with a poor dose rate reconstruction in the age calculation process. The not well bleached grains, which prevents the use of the Al centre. Furthermore, the difficulty of accurately measuring the

Ti-Li signal intensity of natural aliquots (high background noise and baseline), seems to have led to an overestimation of the age obtained using this centre.

For the considered Middle Pleistocene time range (i.e. 700-300 ka), the Ti-H ages are underestimated (Fig. 8) when D_E exceed 300-400Gy, suggesting a saturation of the Ti-H traps. That leads to an underestimation of the ages by comparison with $^{40}Ar/^{39}Ar$. This is verified for our samples except for ESR1 Isoletta sample, for which low dose rate value leads to obtain an age Ti-H older than the $^{40}Ar/^{39}Ar$ age, and for ESR4 Isoletta sample for which a value of about 300 Gy was obtained allowing the calculation of an age close to the $^{40}Ar/^{39}Ar$ one.

It seems therefore preferable to avoid the use of Ti-H centres to date early Middle Pleistocene levels, especially if the D_e derived from Ti-Li and Al centres are greater than 300 Gy. It would be interesting in the future to conduct similar approach, combining $^{40}Ar/^{39}Ar$ and multi-centre ESR, on deposits containing both fluvial quartz and volcanic minerals, from late Middle Pleistocene to Upper Pleistocene (300-50 ka) as well as late Lower Pleistocene times (1.0-0.7 Ma) to further test and validate the MC approach over a longer period of time.

Acknowledgements

We would like to thank the Italian archaeologists and administrative service that are allowed the realization of this study. The present study was financially supported by the project «Acheulean and volcanism in Italy» conducted by M.-H. Moncel (CNRS) and J-.J. Bahain (MNHN) in ATM program (MNHN) «Les dynamiques socio-écosystèmiques, entre perturbations et résiliences environnementales et culturelles», the PHC Galileo project no. 28237WA «l'Acheuléen en Italie méridionale: Chronologie, Paléoanthropologie, Cultures» led by J.-J. Bahain (MNHN) and C. Peretto (University of Ferrara) and the Leakey Foundation supporting the new excavations at Notarchirico led by M-H. Moncel.

The ESR and mobile gamma-ray spectrometers of the French National Museum of Natural History were bought with the financial support of the 'Sesame Île-de-France' program and the 'Région Centre' respectively. We thank the Soprintendenza of Basilicata (Italy) for the agreement to work on the site of

Notarchirico, especially Dr.T.E. Cinquantaquattro, Dr. F. Canestrini, Dr. R. Pirraglia, and Dr. S. Mutino. We also thank the Venosa Museum and Dr. A. Mantrisi for their assistance.

References

Antoine P., Limondin Lozouet N., Chaussé C., Lautridou J.-P., Pastre J.-F., Auguste P., Bahain J.-J., Falguères C.,& Ghaleb B. 2007. Pleistocene fluvial terraces from northern France (Seine, Yonne, Somme): synthesis, and new results from interglacial deposits. Quaternary Science Reviews, 26, 2701–2723

Arnold, L., Stokes, S., Bailey, R., Fattahi, M., Colls, A., Tucker, G. 2003 Optical dating of potassium feldspar using far-red (l>665 nm) IRSL emissions: a comparative study using fluvial sediments from the Loire River, France. Quaternary Science Reviews 22, 1093-1098.

Bartz, M., Rixhon, G., Duval, M., King, G., Alvarez Posada, C., Pares, J., Brückner, H., 2018. Successful combination of electron spin resonance, luminescence and palaeomagnetic dating methods allows reconstruction of the Pleistocene evolution of the lower Moulouya river (NE Morocco). Quaternary Science Reviews, 185, 153-171

Biddittu, I., 1974. Giacimento pleistocenico ad amigdale acheuleane nel territorio di Ceprano, Frosinone. Memoria dell'Istituto Italiano di Paleontologia Umana, 2, 61-67.

Biddittu, I., Canetri, E., Comerci, V., Germani, M., Picchi, G., 2012. Nuove ricerche nel giacimento del Paleolitico inferiore di Lademagne, S. Giovanni Incarico (Frosinone). In: Ghini, G., Mari, Z. (Eds.), Lazio e Sabina. Edizioni Quasar, 9, 437-443

Brennan, B. J., Lyons R.G., Phillips S.W., 1991. Attenuation of alpha particle track dose for spherical grains. Nuclear Tracks Radiation Measurement, 18, 249-253.

Brennan, B. J. 2003, Beta doses to spherical grains. Radiation Measurements 37, 299-303.

Chauhan, P. R., Bridgland, D. R., Moncel, M.-H., Antoine, P., Bahain, J.-J., Briant, R., Cunha, P. P., Despriée, J., Limondin-Lozouet, N., Locht, J.-L., Martins, A. A., Schreve, D. C., Shaw, A. D., Voinchet, P., Westaway, R., White, M. J., White, T. S 2017. Fluvial deposits as an archive of early human activity: Progress during the 20 years of the Fluvial Archives Group. Quaternary Science Reviews. 166, 114-149

Despriée J., Voinchet P., Tissoux H., Bahain J-J., Falguères C., Courcimault G., Dépont J., Moncel M-H., Robin S., Arzarello M., Sala R., Marquer L., Messager E., Puaud S., Abdessadok S., 2011. Lower and Middle Pleistocene human settlements recorded in fluvial deposits of the middle Loire River Basin, Centre Region, France. Quaternary Science Reviews, 30, 11-12, 1474-1485.

Duval, M., Grün, R., Falguères, C., Bahain, J.J., Dolo, J.M., 2009. ESR dating of Lower Pleistocene fossil teeth: Limits of the single saturating exponential (SSE) function for the equivalent dose determination. Radiation Measurements, 44, 477-482.

Duval, M. 2012. Dose response curve of the ESR signal of the Aluminum centre in quartz grains extracted from sediment. Ancient TL 30,1-10

Duval, M., and Guilarte, V., 2015. ESR dosimetry of optically bleached quartz grains extracted from Plio-quaternary sediment: evaluating some key aspects of the ESR signal associated to the Ti-centre. Radiation Measurement, 78, 28–41

Duval, M., Sancho, C., Calle, M., Guilarte, V., Peña-Monné, J.L., 2015. On the interest of using the Multiple Centre approach in ESR dating of optically bleached quartz grains: some examples from the Early Pleistocene terraces of the Alcanadre River (Ebro basin, Spain). Quaternary Geochronology, 29, 58-69. DOI: 10.1016/j.quageo.2015.06.006.

Duval M., Voinchet P., Arnold L.J., Parés J.M., Minnella W., Guilarte V., Demuro M., Falguères C., Bahain J.-J., Despriée J. this issue. A multi-technique dating study of two Lower Palaeolithic sites from the Cher valley (Middle Loire Catchment, France): Lunery-la Terre-des-Sablons and Brinay-la Noira

Grün, R. 1994. A cautionary note: use of the "water content" and "depth for cosmic ray dose rate" in AGE and DATA programs'. Ancient TL, 12, 50-51.

Guérin, G., Mercier, N., Adamiec, G., 2011. Dose-rate conversion factors: update. Ancient TL, 29, 5-8.

Gouveia, M., Cunha, P., Falguères, C., Voinchet, P., Martins, A., Bahain, J.J, Pereira, A. 2020. Electron spin resonance dating of the culminant allostratigraphic unit of the Mondego and Lower Tejo Cenozoic basins (W Iberia), which predates fluvial incision into the basin-fill sediments. Global and Planetary Change, 184.

Kreutzer, S., Duval, M., Bartz, M., Bertran, B., Bosq, M., Eynaud, F., Verdin, F., Mercier, N., 2018. Deciphering long-term coastal dynamics using IR-RF and ESR dating: a case study from Médoc, south-west France, 18, 108-120.

Laurent, M. Falguères C., Bahain, J.J., Yokoyama, Y., 1994. Géochronologie du système de terrasses fluviatiles quaternaires du bassin de la Somme par datation RPE sur quartz, déséquilibres des familles de l'uranium et magnétostratigraphie. C.R. Académie Sciences Paris, 318, 521-526

Laurent, M., Falguères C., Bahain, J.J., Rousseau, L., Van Vliet-Lanoë B., 1998. ESR dating of quartz extracted from Quaternary and Neogene sediments: method, potential and actual limits. Quaternary Science Reviews, 17, 1057-1061.

Lefèvre, D., Raynal, J.P., Vernet, G., Kieffer, G., Piperno, M. 2010. Tephro-stratigraphy and the age of ancient Southern Italian Acheulean settlements: The sites of Loreto and Notarchirico (Venosa, Basilicata, Italy). Quaternary International ; 223–224, 360–368

Ludwig, K.R., 2003, User's Manual for Isoplot/Ex, Version 3.0, A geochronological toolkit for Microsoft Excel Berkeley Geochronology centre . Special Publication, v. 4, Berkeley Geochronology centre, 2455 Ridge Road, Berkeley, CA 94709, USA.

Moncel, M.H., Landais, A., Lebreton, V., Combourieu-Nebout, N., Nomade, S., Bazin, L., 2018. Linking environmental changes with human occupations between 900 and 400 ka in Western Europe.Quaternary International ; 480, 78-94.

Mercier, N., Falguères, C., 2007. Field gamma dose-rate measurement with a NaI(Tl) detector: re-evaluation of the "threshold" technique. Ancient TL, 25,1.

Miallier, D., Sanzelle, S., Falguères, C., Fain, J., Montret, M., Pilleyre, T., Soumana, S., Laurent, M., Gamus, G., De Goër, D., Hervé, A. 1994. Intercomparaison of Tl and ESR signals from heated quartz grains. Radiation measurements, 23, 1, 143-153.

Murray, A.S., Roberts, R.G. 1997. Determining the burial time of single grains of quartz using optically stimulated luminescence. Earth and Planetary Science Letters 152:163-180.

Muttoni, G., Scardia, G., Kent, D. V., 2013. A critique of evidence for human occupation of Europe older than the Jaramillo subchron (~1 Ma): Comment on 'The oldest human fossil in Europe from Orce (Spain)' by Toro-Moyano et al. (2013). Journal of Human Evolution 65, 746-749

Muttoni, G., Scardia, G., Kent, D. V.,2018. Early hominins in Europe: The Galerian migration hypothesis. Quaternary Science Reviews 180, 1-29

574 Niespolo, E.M., Rutte, D., Deino, A., Renne, P.R., 2017. Intercalibration and age of the Alder Creek
575 sanidine 40Ar/39Ar standard. Quaternary Geochronology 39, 205-213.

576 Parés, J.M., Arnold, L., Duval, M., Demuro, M., Pérez-González, A.,Bermúdez de Castro, J.M.,
577 Carbonell, E., Arsuaga, J.L., 2013. Reassessing the age of Atapuerca-TD6 (Spain): new paleomagnetic
578 results Journal of Archaeological Science 40, 4586-4595

579 Pereira A., Nomade S., Voinchet P., Bahain J.-J, Falguères C., Garon H., Lefèvre D., Raynal J.-R.,
580 Scao V., Piperno M., 2015. The earliest securely dated hominin fossil in Italy and evidence of
581 Acheulian occupation during glacial MIS 16 at Notarchirico (Venosa, Basilicata, Italy) Journal
582 Quaternary Science, 30, 7, 639–650.

583 Pereira, A., Nomade, S., Moncel, M.H., Voinchet, P., Bahain, J.J., Biddittu, I., Falgueres, C., Giaccio,
584 B., Manzi, G., Parenti, F., Scardia, G., Scao, V., Sottili G., Vietti, A. 2018. Integrated geochronology
585 of Acheulian sites from the southern Latium (central Italy): Insights on human-environment
586 interaction and the technological innovations during the MIS 11-MIS 10 period Quaternary Science
587 Reviews, 187, 112-129

588 Piperno, M., Mallegni, F., Yokoyama, Y., 1990. Découverte d'un fémur humain dans les niveaux
589 acheuleens de Notarchirico (Venosa, Basilicata, Italie), C. R. Acad. Sc. Paris, 1097–1102
590

591 Piperno, M., Lefèvre., D, Raynal, J.P., Tagliacozzo, A. 1999. Conclusioni generali. In: Notarchirico.
592 Un sito del Pleistocene medio-antico nel bacino di Venosa (Basilicata). Ed. Osanna, Venosa; 537-543

593 Piperno, M., Tagliacozzo, A. 2001. The Elephant Butchery area at the Middle Pleistocene site of
594 Notarchirico (Venosa, Basilicata, Italy). The World of Elephants- International congress, Rome.

595 Prescott, J.R., Hutton, J. T., 1994. Cosmic ray contributions to dose rates for Luminescence and ESR
596 Dating: Large depths and long-term time. Radiation Measurements. 23, 497-500

597 Renne, P.R., Mundil, R., Balco, G., Min, K., Ludwig, K.R., 2011. Joint determination of ^{40}K decay
598 constants and $^{40}Ar/^{40}K$ for the Fish Canyon sanidine standard, and improved accuracy for $^{40}Ar/^{39}Ar$
599 geochronology. Response to the comment by W.H. Schwarz et al. on Geochimica Cosmochimica Acta
600 75, 5097-5100.

601 Rink, W.J., Bartoll, J., Schwarcz, H.P., Shane, P., Bar-Yosef, O., 2007. Testing the reliability of ESR
602 dating of optically exposed buried quartz sediments. Radiation Measurement 42, 1618-1626

603 Sardella, R., Palombo, M.R, Petronio, C., Bedettia, C., Pavi, M. 2006. The early Middle Pleistocene
604 large mammal faunas of Italy: An overview. Quaternary International, 149, 104–109

605 Steiger, R.H., Jäger, E. 1977. Subcommission on geochronology: convention on the use of decay
606 constants in geo and cosmochronology. Earth and Planetary Science Letters 36: 359-362

607 Tissoux, H., Falguères C., Voinchet P., Toyoda S., Bahain J.J., Despriée J. 2007. Potential use of Ti-
608 centre in ESR dating of Fluvial Sediment. Quaternary Geochronology, 2, 1-4, 367-372

609 Tissoux, H., Voinchet, P., Lacquement, F., Prognon, F., Moreno, D., Falguères, C., Bahain, J.-J.,
610 Toyoda S. 2013. Investigation on non-optically bleachable components of ESR aluminium signal in
611 quartz. Radiation Measurements, 47, 9, 894-899

612 Tissoux, H., Voinchet, P., Lerouge, C., 2017. Contribution of cathodoluminescence to the charac-
613 terization and selection of quartz for ESR dating. abstract of LED conference Capetown 2017

614 Toyoda, S. 1991. Production and decay characteristics of paramagnetic defects in quartz: Applications
615 to ESR dating. Ph.D. dissertation, Osaka University, Toyonaka, Osaka, Japan.

Toyoda, S., Falguères C., 2003. The method to represent the ESR signal intensity of the aluminium hole centre in quartz for the purpose of dating. Advances in ESR applications, 20, 7-10.

Toyoda, S., Voinchet, P., Falguères, C., Dolo, J.M. & Laurent, M. 2000. Bleaching of ESR signal by the sunlight: a laboratory experiment for establishing the ESR dating of sediments. Applied Radiation and Isotopes, 52, 5, 1357-1362.

Toyoda, S., Tsukamoto, S., Hameau, S., Usui, H., Suzuki, T. 2006 Dating of Japanese Quaternary tephras by ESR and luminescence methods Quaternary Geochronology, 1, 320–326

Vandenberghe, D., De Corte, F., Buylaert, J.P., Kucera, J., Van den haute, P. 2008. On the internal radioactivity in quartz. Radiation Measurements 43:771-775.

Voinchet, P., Falguères, C., Laurent, M., Toyoda, S., Bahain, J.-J. & Dolo, J.M. 2003. Artificial optical bleaching of the Aluminium centre in quartz implications to ESR dating of sediments. Quaternary Science Reviews, 22, 1335–1338

Voinchet, P., Bahain, J.-J., Falguères, C., Laurent, M., Dolo, J.-M., Despriée, J., Gageonnet R., 2004. ESR dating of quartz extracted from Quaternary sediments: Application to fluvial terraces system of Northern France. Quaternaire, 15, 135-141

Voinchet, P., Falguères, C., Tissoux, H., Bahain, J.J., Despriée J., Pirouelle F. 2007. ESR dating of fluvial quartz: estimate of the minimal distance transport required for getting a maximum optical bleaching. Quaternary Geochronology, 2, 1-4, 363-366

Voinchet P., Despriée J., Tissoux H., Falguères C., Bahain J.-J., Gageonnet R., Dépont J., Dolo J.-M., 2010. ESR chronology of alluvial deposits and first human settlements of the Middle Loire Basin (Region Centre, France). Quaternary Geochronology, 5, 2-3, 381-384

Voinchet, P., Yin, G., Falguères, C., Liu, C., Han, F., Sun, X., Bahain, J.-J. 2013. ESR dose response of Al centre measured in quartz samples from the Yellow River (China): Implications for the dating of Upper Pleistocene sediment. Geochronometria 40, 4, 341-347

Voinchet, P., Toyoda, S., Falguères, C., Hernandez, M., Tissoux, H., Moreno, D., Bahain, J.-J. 2015. Evaluation of ESR residual dose in quartz modern samples, an investigation on environmental dependence. Quaternary Geochronology, 30, 506-512.

Woda, C.A. Wagner, G., 2007. Non-monotonic dose dependence of the Ge and Ti-centres in quartz. Radiation Measurements. 42. 1441-1452.

Yokoyama, Y., Falguères, C., Quaegebeur, J.P., 1985. ESR dating of quartz from Quaternary sediments: first attempt. Nuclear tracks 10, 921–928.

Figures Caption

Fig.1. Location of Isoletta, Lademagne and Notarchirico sites (Italy)

Fig.2. Cross section of Isoletta site and location of ESR and $^{40}Ar/^{39}Ar$ samples– Picture from Biddittu modified.

Fig.3: Cross section of the upper part of Lademagne site and location of $^{40}Ar/^{39}Ar$ and ESR samples

Fig.4: Notarchirico site and location of ESR samples

Fig.5: Stratigraphic sections of Isoletta, Lademagne and Notarchirico sites and $^{40}Ar/^{39}Ar$ results. $^{40}Ar/^{39}Ar$ ages from primary and secondary volcanic deposits from Pereira et al, 2015 and 2018.

Fig 6: Isoletta ESR2 quartz grain ESR spectra (combination of two scans on the 431Gy irradiated aliquot) with Al, Ti-Li an Ti-H signals and indication of the peaks used for the intensity measurements.

Fig.7: Some example of dose response curves obtained for Al, Ti-Li and Ti-H ESR centres. Comparison between De determined using Ti-2 and exponential+linear function for Ti-H centre.

Fig.8: correlation between ESR ages obtained by different paramagnetic centres and $^{40}Ar/^{39}Ar$ ages. Solid line corresponds to the 1:1 ratio. ESR age close to this line (or with error range crossing the line) are considered as accurate, result below this line are underestimated, ages above the line are overestimated.

Fig.SM1: Dose response curves for the different ESR studied centres - Isoletta

Fig.SM2: Dose response curves for the different ESR studied centres - Lademagne and Notarchirico

Tables caption

Tab.1. Radionuclide contents, obtained from High Resolution Gamma Spectrometry, for analyzed sediments of Isoletta, Lademagne and Notarchirico Sites. Analytical uncertainties are given at ± 1σ confidence level.

Tab. 2. ESR results obtained on quartz extracted from sediments. Analytical uncertainties and ages are given with ± 1σ. Water contents (W%) were estimated by the difference in mass between the natural sample and the same sample dried for a week in an oven at 50°C (323.15 K). Dose rates were determined using dose rate conversion factor updated by Guerin et al (2011). Alpha and beta attenuations estimated for the selected grain sizes from the tables of Brennan (2003); k-value of 0.15 (Yokoyama et al., 1985), cosmic dose rate calculated from the equations of Prescott & Hutton (1994). For Ti-H centres, the D_Es and ages marked by an asterisk were calculated using the Ti2 function while the other Ti-H ages and D_Es were calculated using the SSE function. For Ti-Li centres the D_Es and ages in italics were calculated using the SSE function while the other Ti-Li ages and D_Es were calculated using the exponential+linear function.

Tab. 3. Isoletta Site, Comparison between ESR and $^{40}Ar/^{39}Ar$ ages. $^{40}Ar/^{39}Ar$ ages are given with 2σ analytical uncertainty and are already published in Pereira et al 2018. Ti-H ages are used for mean ages calculation of ESR 3 and 4.

Tab. 4. Lademagne Site, Comparison between ESR and $^{40}Ar/^{39}Ar$ ages; $^{40}Ar/^{39}Ar$ ages are given with 2σ analytical uncertainty and are already published in Pereira et al 2018.

Tab. 5 Notarchirico Site, Comparison between ESR and $^{40}Ar/^{39}Ar$ ages. $^{40}Ar/^{39}Ar$ ages are given with 2σ analytical uncertainty and are already published in Pereira et al 2015. Ti-H ages are not used for mean age calculation.

703

	U(ppm)	Th (ppm)	K (%)
Isoletta ESR1	1.58 ± 0.07	0.31 ± 0.07	0.03 ± 0.01
Isoletta ESR2	1.62 ± 0.14	9.37 ± 0.22	2.39 ± 0.03
Isoletta ESR 3	1.79 ± 0.09	2.43 ± 0.13	0.44 ± 0.01
Isoletta ESR 4	1,40 ± 0,06	1.07 ± 0.07	0.23 ± 0.01
Lademagne Upper	1.04 ± 0.11	2.91 ± 0.06	0.80 ± 0.02
Notarchirico 2-6	4.69 ± 0.08	4.87 ± 0.04	1.45 ± 0.01
Notarchirico H1	2.72 ± 0.08	4.48 ± 0.04	0.83 ± 0.01
Notarchirico H1-c	3.22 ± 0.09	5.89 ± 0.05	1.07 ± 0.01

Tab.1. Radionuclide contents, obtained with High Resolution Gamma Spectrometry, for analyzed sediments of Isoletta, Lademagne and Notarchirico Sites. Analytical uncertainties are given at ± 1σ confidence level.

		D_α µGy/a	D_β µGy/a	D_γ µGy/a	D_{cos} µGy/a	D_A µGy/a	W %	Bl %	D_E (Gy)	r^2	Age (ka)
Isoletta											
ESR1	Al	19±1	190±11	168±10	24±1	401±15	15	48	462 ± 24	0.992	1154 ± 109
	Ti-Li							100	715 ± 75 *803 ±100*	0.986 *0.981*	1786 ± 327
	Ti-H								325 ± 29 298 ± 22*	0.981 0.987*	810 ± 47 743 ± 40*
ESR2	Al	57±2	1786±36	1008±28	33±1	2884±15	15	42	1315 ± 62	0.991	456 ± 34
	Ti-Li							100	1155 ± 110 *1059±120*	0.989 *0.979*	401 ± 59
	Ti-H								295 ± 20 302 ± 20*	0.991 0.989*	102 ± 16 105 ± 15
ESR3	Al	30±2	497±20	354±16	53±3	934±26	15	46	338 ± 60	0.981	362 ± 64
	Ti-Li							100	314 ± 73 *401 ±45*	0.979 *0.987*	336 ± 66
	Ti-H								349 ± 24 288 ± 12*	0.988 0.990*	374 ± 17 308 ± 22*
ESR4	Al	20±1	303±12	220±10	101±5	644±16	15	44	252 ± 40	0.984	391 ± 72
	Ti-Li							100	275 ± 25 *296 ±38*	0.989 *0.984*	426 ± 59
	Ti-H								243 ± 15 230 ± 22*	0.987 0.989*	377 ± 84 357 ± 81*
Lademagne											
Lad Sup	Al	77±3	980±35	919±52	111±6	2087±70	5	44	847±100	0.981	406±51
	Ti-Li							100	831±70 *875 ±88*	0.985 *0.989*	398±51
Notarchirico											
2-6	Al	84±1	1999±24	1803±21	166±8	4052±32	10	57	2658±122	0.991	657±31
H1	Al	115±2	1203±20	1215±18	95±5	2628±27	17	66	1942±60	0.995	739±43
	Ti-Li							100	1972±110 *1895±161*	0.995 *0.989*	750±57
	Ti-H								312 ± 21 330 ± 28*	0.992 0.985*	119 ±35 125 ± 38*
H1-c	Al	146±2	1521±23	1551±22	95±5	3313±32	17	69	2425±85	0.993	732±49
	Ti-Li							100	2453±100 *2515 ±200*	0.989 *0.991*	740 ±52
	Ti-H								887± 71 810 ± 82*	0.981 0.978*	267± 28 245 ± 26*

Tab. 2. ESR results obtained on quartz extracted from sediments. Analytical uncertainties and ages are given with ± 1σ. Water contents (W%) were estimated by the difference in mass between the natural sample and the same sample dried for a week in an oven at 50°C (323.15 K). Dose rates were determined using dose rate conversion factor updated by Guerin et al (2011). Alpha and beta attenuations estimated for the selected grain sizes from the tables of Brennan (2003); k-value of 0.15 (Yokoyama et al., 1985), cosmic dose rate calculated from the equations of Prescott & Hutton (1994). For Ti-H centres, the D_Es and ages marked by an asterisk were calculated using the Ti2 function while the other Ti-H ages and D_Es were calculated using the SSE function. For Ti-Li centres the D_Es and ages in italics were calculated using the SSE function while the other Ti-Li ages and D_Es were calculated using the exponential+linear function.

	Al ESR ages	Ti-Li ESR ages	Ti-H ESR ages	Mean ESR ages	$^{40}Ar/^{39}Ar$ ages
ESR1	1154±109ka	1786 ± 327 ka	810 ± 47 ka	Not possible	403 ± 8 ka
ESR2	456 ± 34 ka	401 ± 59 ka	102 ± 16 ka	442 ± 58 ka	375 ± 10 ka
ESR3	362 ± 64 ka	336 ± 66 ka	374 ± 17 ka	349 ± 26 ka	365 < expected < 375
ESR4	391 ± 72 ka	426 ± 59 ka	377 ± 84 ka	396 ± 83 ka	365 ± 19 ka

Tab. 3. Isoletta Site, Comparison between ESR and $^{40}Ar/^{39}Ar$ ages. $^{40}Ar/^{39}Ar$ ages are given with 2σ analytical uncertainty and are already published in Pereira et al 2018. Ti-H ages are used for mean ages calculation of ESR 3 and 4.

	Al ESR age	Ti-Li ESR age	Mean ESR age	Ti-H ESR age	$^{40}Ar/^{39}Ar$ age
Lad Sup	406 ± 51 ka	398 ± 51 ka	402 ± 71 ka	inapplicable	389 ± 8 ka

Tab. 4. Lademagne Site, Comparison between ESR and $^{40}Ar/^{39}Ar$ ages; $^{40}Ar/^{39}Ar$ ages are given with 2σ analytical uncertainty and are already published in Pereira et al 2018.

	Al ESR ages	Ti-Li ESR ages	Mean ESR ages	TiH ESR ages	$^{40}Ar/^{39}Ar$ ages
Notarchirico 2-6	657 ± 31 ka	-	-	-	663 ± 13 ka
Notarchirico H1	739±43 ka	750±57 ka	743 ± 67 ka	119 ± 35 ka	> 670 ± 14 ka
Notarchirico H1c	732±49 ka	740 ±52 ka	736 ± 70 ka	267 ± 28 ka	> 670 ± 14 ka

Tab. 5 Notarchirico Site, Comparison between ESR and $^{40}Ar/^{39}Ar$ ages. $^{40}Ar/^{39}Ar$ ages are given with 2σ analytical uncertainty and are already published in Pereira et al 2015. Ti-H ages are not used for mean age calculation.

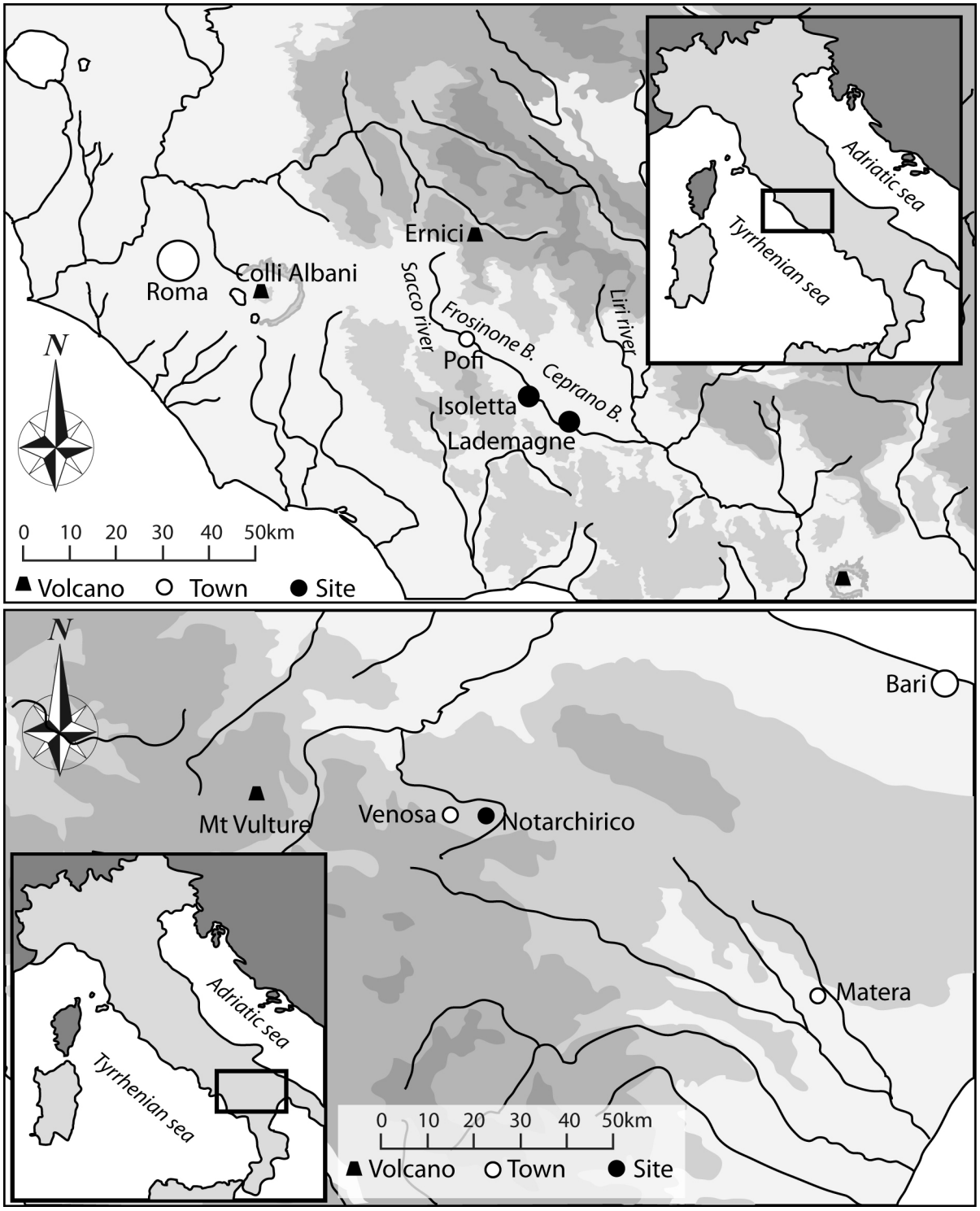
Roma
Colli Albani
Ernici
Sacco river
Frosinone B.
Ceprano B.
Liri river
Posi
Isoletta
Lademagne
Adriatic sea
Tyrrhenian sea
N
0 10 20 30 40 50km
Volcano
Town
Site
Bari
Mt Vulture
Venosa
Notarchirico
Matera